Biochimica et Biophysica Acta 1848 (2015) 1139–1146

Contents lists available at ScienceDirect

Biochimica et Biophysica Acta

journal homepage: www.elsevier.com/locate/bbamem

Antimicrobial properties of membrane-active dodecapeptides derived from MSI-78☆

Claudia Monteiro [a,b,1], Mariana Fernandes [a,b,1], Marina Pinheiro [c,1], Sílvia Maia [d], Catarina L. Seabra [a,b,e,f], Frederico Ferreira-da-Silva [a,g], Fabíola Costa [a,b,h], Salette Reis [c], Paula Gomes [d], M. Cristina L. Martins [a,b,e,*]

[a] I3S, Instituto de Investigação e Inovação em Saúde, Universidade do Porto, Portugal
[b] INEB — Instituto de Engenharia Biomédica, Universidade do Porto, Rua do Campo Alegre 823, 4150-180 Porto, Portugal
[c] Requimte, Faculdade de Farmácia, Universidade do Porto, Rua de Jorge Viterbo Ferreira 228, 4050-313 Porto, Portugal
[d] CIQUP, Departamento de Química e Bioquímica, Faculdade de Ciências, Universidade do Porto, Rua do Campo Alegre 687, 4169-007 Porto, Portugal
[e] ICBAS — Instituto de Ciências Biomédicas Abel Salazar, Universidade do Porto, Rua de Jorge Viterbo Ferreira 228, 4050-313 Porto, Portugal
[f] IPATIMUP — Institute of Molecular Pathology and Immunology of the University of Porto, Rua Dr. Roberto Frias, 4200-465 Porto, Portugal
[g] IBMC — Instituto de Biologia Celular e Molecular, Unidade de Produção e Purificação de Proteínas, Universidade do Porto, Rua do Campo Alegre 823, 4150-180 Porto, Portugal
[h] Faculdade de Engenharia, Universidade do Porto, Rua Dr. Roberto Frias s/n, 4200-465 Porto, Portugal

ARTICLE INFO

Article history:
Received 4 September 2014
Received in revised form 14 December 2014
Accepted 3 February 2015
Available online 10 February 2015

Keywords:
Antimicrobial peptide
MSI-78
Pexiganan
Antibiotic resistance
Cytotoxicity
Membrane model

ABSTRACT

Antimicrobial peptides (AMPs) are a class of broad-spectrum antibiotics known by their ability to disrupt bacterial membranes and their low tendency to induce bacterial resistance, arising as excellent candidates to fight bacterial infections. In this study we aimed at designing short 12-mer AMPs, derived from a highly effective and broad spectrum synthetic AMP, MSI-78 (22 residues), by truncating this peptide at the *N*- and/or *C*-termini while spanning its entire sequence with 1 amino acid (aa) shifts. These designed peptides were evaluated regarding antimicrobial activity against selected gram-positive *Staphylococcus* strains and the gram-negative *Pseudomonas aeruginosa* (*P. aeruginosa*).

The short 12-mer peptide CEM1 (GIGKFLKKAKKF) was identified as an excellent candidate to fight *P. aeruginosa* infections as it displays antimicrobial activity against this strain and selectivity, with negligible toxicity to mammalian cells even at high concentrations. However, in general most of the short 12-mer peptides tested showed a reduction in antimicrobial activity, an effect that was more pronounced for gram-positive *Staphylococcus* strains. Interestingly, CEM1 and a highly similar peptide differing by only one aa-shift (CEM2: IGKFLKKAKKFG), showed a remarkably contrasting AMP activity. These two peptides were chosen for a more detailed study regarding their mechanism of action, using several biophysical assays and simple membrane models that mimic the mammalian and bacterial lipid composition.

We confirmed the correlation between peptide helicity and antimicrobial activity and propose a mechanism of action based on the disruption of the bacterial membrane permeability barrier.

© 2015 Elsevier B.V. All rights reserved.

1. Introduction

Resistance to antibiotics is becoming a huge threat to public health [1], thus new efforts are warranted in order to find alternative therapeutic solutions. Among these, antimicrobial peptides (AMPs) have been described as a promising new class of antibiotics and are nowadays considered the most innovative anti-infective agents of the last decades [2–4].

AMPs are part of the innate immune system of several organisms such as animals, plants, fungi, bacteria and viruses. These peptides are usually 10–50 residues in length, highly cationic and have tendency to form amphipathic structures, mostly due to the presence of separate hydrophobic and cationic domains [5,6]. Electrostatic attraction between the cationic AMPs and anionic lipids of bacterial membranes promotes the first interactions. Most AMPs seem to kill bacteria by compromising membrane integrity through direct binding to the lipid bilayer [7,8].

MSI-78 (commercially known as Pexiganan), a 22-mer AMP developed for the treatment of infected diabetic foot ulcers [9,10], is a broad spectrum AMP effective against over 3000 clinical isolates including methicillin and gentamicin-resistant *Staphylococcus aureus* (*S. aureus*) [9,11]. Practically no resistance has been associated to this highly potent AMP [9,10,12].

MSI-78 has been described to disrupt bacterial membranes via a toroidal-type pore formation upon binding to the membrane, forming an antiparallel dimer of amphipathic helices [11]. The α-helical

☆ No benefit of any kind will be received either directly or indirectly by the authors.

* Corresponding author at: INEB — Instituto de Engenharia Biomédica, Rua do Campo Alegre 823, 4150-180 Porto, Portugal. Tel.: +351 22 6074982; fax: +351 22 6094567.
E-mail address: cmartins@ineb.up.pt (M.C.L. Martins).

[1] These authors contributed equally to this work.

http://dx.doi.org/10.1016/j.bbamem.2015.02.001
0005-2736/© 2015 Elsevier B.V. All rights reserved.

arrangement, although not sufficient for antimicrobial activity, is recognized to favor AMP insertion in the microorganism membrane, as the peptide amphipathic conformation allows the insertion of a well-defined hydrophobic sector into the lipid bilayer [13].

Although AMPs are promising antibiotic alternatives, they still present a few drawbacks that compromise their therapeutic application such as: low stability, high toxicity and high production costs [14]. Moreover the typical macromolecular size of AMP (20–40 amino acids (aa)) limits the administration routes to topical and parenteral ones, impairing a wide pharmaceutical applicability [15]. Therefore short AMPs with high selectivity towards bacterial cells are desirable candidates. The rational shortening of natural AMPs while maintaining antimicrobial activity has been successfully done before with cecropin A-Mellitin hybrids [16,17] and could be a strategy to tackle some of the aforementioned drawbacks such as high toxicity and cost of production while improving AMP therapeutic index.

With this work we aimed at the synthesis and study of new short AMPs, namely, 12-mer fragments based on MSI-78, which were designed to span the MSI-78 sequence with 1 aa shifts, while attempting to preserve its remarkable features (Table 1).

Antimicrobial activity studies, using gram-positive *Staphylococcus* strains and the gram-negative *Pseudomonas aeruginosa* (*P. aeruginosa*), revealed differential efficiencies between the eleven 12-mer peptides synthesized. Interestingly, two highly similar peptides differing by only one aa-shift, showed a remarkably contrasting AMP activity, one being the most effective peptide synthesized. These two peptides were chosen for a more detailed study regarding their mechanism of action, using several biophysical assays, and simple membrane models that mimic the mammalian and bacterial lipid composition. In this study, large unilamellar vesicles (LUVs) were used as membrane models since they simulate an environment identical to biological membranes, *i.e.* they are anisotropic and possess both lipophilic and hydrophilic regions. In addition, LUVs are comparatively more stable and can be easily quantified in terms of lipid concentration, surface area and volume than model systems such as lipid mixture suspensions, lipid films, and small unilamellar vesicles [18,19]. Since phosphatidylcholines are generally the most abundant phospholipids in mammalian plasma membranes [20], 1,2-dimyristoyl-*sn*-glycero-phosphocholine (DMPC), a zwitterionic phospholipid, was chosen [20,21] to mimic the neutral mammalian cell membrane. On the other hand, phosphatidylglycerols are abundant in bacterial membranes [22,23], therefore the 1,2-dimyristoyl-*sn*-glycero-3-phosphoglycerol (DMPG), a negatively charged phospholipid, was used as the membrane model of the bacterial cell membrane.

2. Materials and methods

2.1. Reagents

N^{α}-Fmoc-protected amino acids, Rink amide AM resin, and 2-(1H-Benzotriazole-1-yl)-1,1,3,3-tetramethyluronium hexafluorophosphate (HBTU) for solid phase peptide synthesis (SPPS) were from NovaBiochem-EMD4Biosciences (Darmstadt, Germany). *N*-ethyl-*N*,*N*-diisopropylamine (DIEA), 1-hydroxybenzotriazole (HOBt), trifluoroacetic acid (TFA), triisopropylsilane (TIS), piperidine and all solvents for SPPS were from Sigma-Aldrich (St. Louis, MO, USA). Octadecylsilane stationary phase 238TPB1520 for peptide purification by medium-pressure reverse-phase liquid chromatography (MP-RPLC) was from Vydac (Hesperia, CA, USA). The lipids, 1,2-dimyristoyl-*sn*-glycero-3-phosphocholine (DMPC) and 1,2-dimyristoyl-*sn*-glycero-3-phosphoglycerol (DMPG) were also purchased from Sigma-Aldrich Co. (St. Louis, MO, USA). Hepes buffer used in the biophysical experiments with LUV consisted of 10 mmol L^{-1} *N*-(2-hydroxyethyl)piperazine-*N*′-(2-ethanesulfonic acid), the ionic strength was adjusted to 0.1 M with sodium chloride and the pH to 7.4. In the circular dichroism (CD) experiments, the buffer consisted of 10 mmol L^{-1} of sodium buffer and the ionic strength was adjusted to 0.1 M with sodium fluoride and the pH to 7.4. Hepes and sodium phosphate buffer were supplied by Sigma-Aldrich Co. (St. Louis, MO, USA). All the other chemicals were purchased from Merck.

2.2. Peptide synthesis and characterization

All peptides (Table 1) were prepared as *C*-terminal amides by standard Fmoc/^{t}Bu SPPS on a Liberty1 Microwave (MW) Peptide Synthesizer (CEM Corporation, Mathews, NC, USA) [24]. Briefly, Rink amide AM resin was pre-swelled for 15 min in *N*,*N*-dimethylformamide (DMF) and then transferred into the MW-reaction vessel. The initial Fmoc deprotection step was carried out using 20% piperidine in DMF containing 0.1 M HOBt in two MW irradiation pulses: 30 s at 24 W plus 3 min at 28 W, in both cases the temperature being no higher than 75 °C. The Fmoc-protected *C*-terminal amino acid (Bachem, Switzerland) was then coupled to the resin, using 5 molar equivalents (eq) of the Fmoc-protected amino acid in DMF (0.2 M), 5 eq of 0.5 M HBTU/HOBt in DMF and 10 eq of 2 M DIEA in *N*-methylpyrrolidone (NMP); the coupling step was carried out for 5 min at 35 W MW irradiation, with maximum temperature reaching 75 °C. The remaining amino acids were sequentially coupled in the C → N direction by means of similar deprotection and coupling cycles. Following completion of sequence assembly, the peptides were released from the resin with concomitant removal of side-chain protecting groups, by a 3 h-acidolysis at room temperature using a TFA-based cocktail containing TIS and water as scavengers (TFA/TIS/H_2O 95:2.5:2.5 v/v/v). Crude products were purified by MP-RPLC to a purity of at least 95%, as confirmed by high-performance liquid chromatography (HPLC) analysis on a Hitachi-Merck LaChrom Elite system equipped with a quaternary pump, a thermostated (Peltier effect) automated sampler and a diode-array detector (DAD). Pure peptides were quantified by UV-absorption spectroscopy (Helios Gama, Spectronic Unicam) and their molecular weights confirmed to be as expected by electrospray ionization/ion trap mass spectroscopy (ESI/IT MS; LCQ-DecaXP LC-MS system, ThermoFinnigan).

Table 1
Amino acid sequences and selected features of synthetic peptides derived from MSI-78. The 12-mer peptides were designed to span MSI-78 by 1-residue shift.

Peptides	Amino acid sequence	Molecular weight	Charge	Total hydrophobic ratio	Aliphatic index
MSI-78	GIGKFLKKAKKFGKAFVKILKK 22 aa	2476	+9	45%	93.18
CEM1	GIGKFLKKAKKF 12 aa	1363,80	+5	41%	73.33
CEM2	IGKFLKKAKKFG	1363,73	+5	41%	73.33
CEM3	GKFLKKAKKFGK	1378,86	+6	33%	40.83
CEM4	KFLKKAKKFGKA	1392,73	+6	41%	49.17
CEM5	FLKKAKKFGKAF	1411,73	+5	50%	49.17
CEM6	LKKAKKFGKAFV	1363,73	+5	50%	73.33
CEM7	KKAKKFGKAFVK	1378,73	+6	41%	40.83
CEM8	KAKKFGKAFVKI	1363,67	+5	50%	73.33
CEM9	AKKFGKAFVKIL	1348,80	+4	58%	105.83
CEM10	KKFGKAFVKILK	1405,82	+5	50%	97.50
CEM11	KFGKAFVKILKK	1405,82	+5	50%	97.50

2.3. Antimicrobial activity prediction studies

The Collection of Antimicrobial Peptides (CAMP) (http://www.bicnirrh.res.in/antimicrobial/) was selected based on the number of included peptide sequences, manual validation, variety of peptide origins and prediction tools offer. Peptide sequence features analyzed were: i) antimicrobial probability assessed by three different algorithms &&(Random Forest (RF), Support Vector Machines (SVM) and Discriminant Analysis (DA)); ii) overall net charge; iii) % hydrophobic residues and iv) aliphatic index (the aliphatic index of a protein is defined as the relative volume occupied by aliphatic side chains, i.e., from alanine, valine, isoleucine, and leucine).

2.4. Microorganisms and growth conditions

Microorganisms tested in this study were the following: *S. aureus* ATCC 33591 (methicillin resistant), *S. aureus* ATCC 25923, *P. aeruginosa* ATCC 27853, *Staphylococcus epidermidis* (*S. epidermidis*) ATCC 35984 and *Candida albicans* (*C. albicans*) DSM 1386. Bacteria were grown on Trypticase Soy Agar (TSA) plates and Mueller–Hinton broth (MHB). *C. albicans* was grown on Sabouraud Maltose agar (SMA), Sabouraud Dextrose broth (SDB) and RPMI 1640 with 3-(-morpholino)propanesulfonic acid (MOPS), with L-glutamine and without sodium hydroxide.

2.5. Antimicrobial testing

Antimicrobial activity was assessed by Minimal Inhibitory Concentration (MIC) and Minimal Bactericidal Concentration (MBC). The method used to determine the MIC was the broth microdilution assay in microtiter plates, described by Wiegand and co-workers [25]. This method follows the guidelines of the two recognized organizations, CLSI and EUCAST. Bacteria were pre-cultured on TSB overnight at 37 °C and 150 rpm. After washing with phosphate buffered saline (PBS) bacteria were adjusted to approximately 2×10^5 CFU/mL in MHB and 99 μL was transferred to a 96 well plate. *C. albicans* was inoculated in SDB for 16 h at 37 °C in an orbital shaker at 120 rpm. After washing with PBS cell number was adjusted to 1.6×10^6 cells/mL in RPMI medium using an improved Neubauer hemocytometer and 99 μL was transferred to a 96 well plate. Polypropylene microtiter plates were used to prevent binding of the peptides to the walls of the wells. Peptide dilutions were prepared in acetic acid/bovine serum albumin (BSA) solution and peptide concentrations tested ranged from 512 μg/mL to 0.015 μg/mL, adjusted according to results obtained in preliminary experiments. The peptides were tested in a final volume of 110 μL.

The minimum bactericidal concentrations (MBC) were determined by plating the content of the first three wells where visible growth was not observed.

2.6. Hemolysis assay on human red blood cells (RBC)

Human blood buffy coats were obtained from healthy volunteers (Centro Hospitalar de São João, EPE, Porto, Portugal) and processed to obtain RBC by centrifugation over density gradient with Histopaque-1077 Sigma-Aldrich Co. (St. Louis, MO, USA) according to the manufacturer's instructions. After removal of the plasma upper layer, the lower layer containing RBC was washed three times in PBS. The purified RBC were diluted to $6–7 \times 10^8$ cells/mL in PBS and 99 μL was distributed in a 96 well polypropylene microtiter plate.

Peptide dilutions were prepared in acetic acid/BSA solution and the range of peptide concentrations tested went from 512 μg/mL to 1 μg/mL. After 1 h of incubation at 37 °C under 5% CO_2, cells were centrifuged at 900 *g* for 10 min and the supernatant was transferred to a 96 well plate. The absorbance values of the released hemoglobin were determined at 450 nm using a microplate reader (Synergy Mx, Biotek). Untreated cells were used as negative control and cells treated with 0.2% Triton X-100 as positive controls. The percentage hemolysis was calculated as ((sample absorbance − negative control absorbance) / (positive control absorbance − negative control absorbance)) × 100.

2.7. Preparation of cell membrane models — large unilamellar vesicles (LUVs)

Lipid films were formed from chloroform solution of DMPC and DMPG lipids, dried under a stream of nitrogen and left under reduced pressure for a minimum of 45 min, to remove all traces of the organic solvent. LUVs were prepared by the addition of the buffer, followed by vortexing which yields multilamellar vesicles (MLV). Lipid suspensions were equilibrated at 37.0 ± 0.1 °C for 30 min and extruded 10 times through polycarbonate filters with a diameter pore of 100 nm to form LUV as previously described [20].

2.8. Circular dichroism (CD) analysis

The secondary structure of the peptides CEM1, CEM2 and MSI-78, was investigated using CD on a JASCO J-815 spectropolarimeter, equipped with a temperature-controlled cuvette and controlled by the Spectra manager software.

Peptide solutions were diluted in 10 mM sodium phosphate, pH 7.4, 100 mM sodium fluoride to a concentration of 40 μM with and without 5 mM DMPG or DMPC LUV, corresponding to peptide:lipid molar ratio of 1:125.

Before the measurement all peptide solutions were incubated at 37 °C for 30 min.

Far-UV CD spectra were recorded between 195 and 260 nm using a 1 mm path length cuvette. CD spectra were acquired with a scanning speed of 100 nm/min, an integration time of 1 s, and using a bandwidth of 1 nm. The spectra were averaged over sixteen scans and corrected by subtraction of the buffer signal.

The results are expressed as the mean residue ellipticity $_{MRW}$, defined as $_{MRW} = {}_{obs}(0.1MRW)/(lc)$, where $_{obs}$ is the observed ellipticity in millidegrees, MRW is the mean residue weight, c is the concentration in mg/mL and l is the light path length in cm.

The mean helix content (f_H) was calculated according to Luo and Baldwin [26]. Briefly, f_H is obtained from the $_{MRW}$ at 222 nm of each peptide ($_{222}$) according to the equation: $f_H = ({}_{222} - {}_{C})/({}_{H} - {}_{C})$, where the baseline ellipticities for random coil ($_C$) and complete helix ($_H$) are given by: $_C = 2220 - 53T$ and $_H = (-44000 + 250T)(1 - 3/N)$, where T is the temperature in °C and N is the chain length in number of residues.

2.9. Hydrodynamic diameter and ζ-potential of LUV

The hydrodynamic diameters of the LUV in the absence and in the presence of AMP were determined in BI-MAS dynamic light scattering (DLS) instrument (Brookhaven Instruments, USA). Typically 6 runs (2 min each) were performed and the cumulate analysis was applied to scattering data to give effective diameters and polydispersity. The ζ-potential was assessed through the determination of the electrophoretic mobility using a ZetaPALS (Brookhaven Instruments Corporation). For both determinations the temperature was maintained at 37.0 ± 0.1 °C, being the lipid concentration kept constant at 500 μM, and AMP concentration ranged from 0–40 μM (0, 5, 10, 20 and 40 μM).

2.10. Biophysical properties of LUV

The effects of AMP (7.3 and 40 μM) on the biophysical parameters (T_m and cooperativity) of DMPC and DMPG LUV (500 μM) were determined by DLS [27]. The count rate was obtained using a BI-MAS DLS instrument (Brookhaven Instruments, USA), containing a controlled temperature cell holder. The samples were heated from 10.0 ± 0.1 °C to 40.0 ± 0.1 °C with intervals of 1.0 ± 0.1 °C and with an equilibration period of 2 min. At each temperature, six 2-min runs were performed.

The discontinuity in the mean count rate (average number of photons detected per second) as the temperature changes, corresponds to an alteration in the optical properties of the material studied (*i.e.*, transition from initial state to another one) [28]. Data as the normalized mean count rate versus temperature were collected and fitted using:

$$r_s = r_{s1} + p_1 T + \frac{r_{s2} - r_{s1} + p_2 t - p_1 T}{1 + 10^{B(1/T - 1/T_m)}} \quad (1)$$

where r_s is the average count rate, T is the temperature (°C), p_1 and p_2 correspond to the slopes of the straight lines at the beginning and at the end of the plot, and r_{s1} and r_{s2} are the respective count rates intercepting the values at the y axis [28]. From the experimental data displayed, it was possible to calculate the cooperativity (B) and the midpoint of the phase transition, which corresponds to the temperature of the gel-to-fluid phase transition of the lipid (T_m) [28]. The T_m was calculated from the slope and the inflection point of the data fitted to sigmoid curves of count rate (r_s) versus temperature (T) [27].

3. Results

3.1. Peptide design

The eleven MSI-78-based 12-mer peptides synthesized are described in Table 1. The 12-mer length was chosen as optimal regarding biological function as, while short, it still allows peptide folding as amphipathic α-helices, as occurs with the lead peptide MSI-78 when exerting its antimicrobial action [11].

In order to have a preliminary insight on the overall impact of the truncations on the antimicrobial properties of the 12-mers, AMP predictions and particular structure properties that have been related to antimicrobial activity were analyzed using the AMP prediction tools of CAMP. According to prediction outcomes all CEM peptides were classified as AMPs. All the peptides equally displayed adequate charge for an AMP, as the majority of natural AMPs have a net charge from +4 to +9 [29]. Hydrophobic ratios between 40%–60% have been found in natural AMPs, and all CEM peptides are in this range with the exception of CEM3 with a 33% hydrophobic ratio [29].

As antimicrobial prediction and key features were indicative of antimicrobial activity by all designed CEM peptides, a screening of the peptides was made in order to find and study one or more short peptides that could best preserve MSI-78 antimicrobial properties while providing indications on future strategies for the rational design of short, truncated AMPs.

3.2. Antimicrobial characterization

MIC of MSI-78 and its 12-mer derivatives against *S. aureus*, *S. epidermidis*, and *P. aeruginosa* are described in Table 2. Regarding gram-positive bacteria, and as compared to the lead MSI-78 peptide, the 12-mers lost activity against both *S. aureus* strains tested, independently from their resistance to methicillin. Only the peptides that cover the *C*-terminus of MSI-78 (CEM9, CEM10 and CEM11) showed some antimicrobial activity at high concentrations against these bacteria.

S. epidermidis was in general more susceptible to the 12-mers than *S. aureus* strains, with several peptides having MIC values below 512 μg/mL. CEM1 with a MIC of 32–64 μg/mL was the most effective 12-mer against this bacterium.

Regarding the gram-negative bacteria *P. aeruginosa* MIC values demonstrate that this strain is much more susceptible to the CEM 12-mers and to MSI-78 than the tested gram-positive strains (*Staphylococcus* strains), with some peptides having relatively low MIC (CEM1, CEM5, CEM9, CEM10 and CEM11). As previously shown for *S. epidermidis*, CEM1 was again the most effective peptide against *P. aeruginosa* with a MIC of 4–8 μg/mL.

Table 2
Determination of minimum inhibitory concentrations of MSI-78 and 12-mer derivatives against selected microorganisms.

	Microorganisms			
Peptides	*S. aureus* (MRSA)	*S. aureus*	*S. epidermidis*	*P. aeruginosa*
MSI-78	16–32	8–16	0.5–1 (0.2–0.4)	0.5–1 (0.2–0.4)
CEM1	>512	512	32–64 (23–47)	4–8 (2.9–5.7)
CEM2	>512	>512	256 (194)	128–256 (94–194)
CEM3	>512	>512	256–512	>512
CEM4	>512	>512	512–>512	512
CEM5	>512	>512	256	64
CEM6	>512	>512	>512	256–512
CEM7	512	>512	>512	>512
CEM8	>512	>512	128–256	64–128
CEM9	128	256	128	32–64
CEM10	256	256	64–128	16–32
CEM11	256–512	256–512	64–128	16–32

MIC values are presented in μg/mL. Concentrations in μM are in parenthesis.

MBC results (data not shown) were the same range or two fold higher than MIC, indicating bactericidal effect of the peptides for the concentrations tested.

Regarding the fungus strain, MSI-78 peptide did not show any effect against *C. albicans* DMS 1386 at the concentrations tested, although published data reports antifungal activity for MSI-78 [30]. Therefore 12-mer peptides were not tested against *C. albicans*.

MSI-78 activity was in general comparable to previously published studies, being effective at low concentrations against *S. aureus*, *S. epidermidis* and *P. aeruginosa*. MIC values obtained for MSI-78 against *S. aureus* are in agreement with published data, results for *S. epidermidis* and *P. aeruginosa* 27853 are slightly lower than published data, however MIC of MSI-78 against these strains varies in the literature [9,11,30].

3.3. Cytotoxicity

Cytotoxicity studies were performed with CEM1, the selected AMP that maintained high antimicrobial activity against *P. aeruginosa* and *S. epidermidis*, and CEM2 that, despite differing only by 1 aa-shift from the active peptide, had significantly diminished antimicrobial activity.

CEM1 and CEM2 were less cytotoxic to RBC than the reference AMP, MSI-78 (Fig. 1). MSI-78 showed some toxicity at high concentrations (53% hemolysis at 512 μg/mL, 25% hemolysis at 256 μg/mL and 13% hemolysis at 128 μg/mL), which is in agreement with data published before [31]. The short peptides, CEM1 and CEM2, showed no toxicity to RBC even at the higher concentrations tested.

3.4. CD analysis

CD spectra of the parent peptide MSI-78, CEM1 and CEM2 in aqueous buffer exhibited a negative minimum at ≈198 nm suggesting random coil conformations. In the presence of DMPC LUV, spectra also exhibit characteristic profiles of unordered peptides, pointing out to no toxicity towards mammalian cells. In the presence of DMPG LUV, two negative minima at ≈208 nm and ≈222 nm suggest the presence of α-helical conformations (Fig. 2). For all the peptides, results indicate a transition from a random coil to an ordered secondary structure upon interaction with the bacterial membrane mimetic system DMPG LUV. In presence of DMPG LUV, calculated mean helix contents show differences between the peptides. The parent 22-mer peptide MSI-78 has 61% helicity, whereas helicity values around 40–45% have been reported by Mercke et al. for this peptide when bound to 1-palmitoyl-2-oleoyl-sn-glycero-3-phosphocholine (POPC) small unilamellar vesicles [32,33]. For the 12-mers the mean helix content determined was 53% for CEM1 and 35% for CEM2. This result shows a difference of about 20% in the helix content between the two peptides, which may explain their differential interaction with bacterial cells. Interestingly, while having the same number and composition of aa, the only difference in

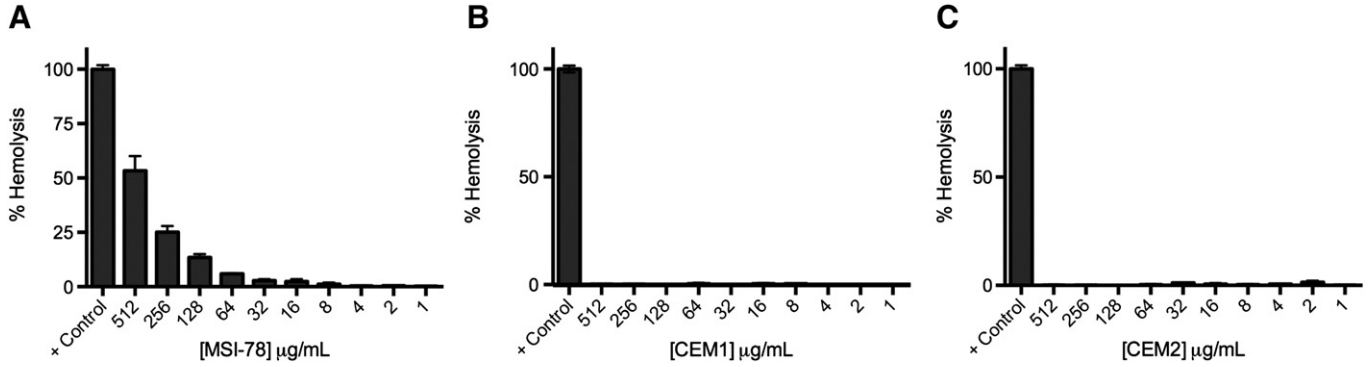

Fig. 1. Hemolytic activity of (A) MSI-78, (B) CEM1 and (C) CEM2 on human red blood cells. Peptide concentrations tested covered a range from 512 μg/mL to 1 μg/mL. Untreated bacterial cells were used as negative control and bacterial cells treated with 0.2% Triton X-100 were used as positive control.

their primary structures comes from the position of a glycine residue which is at the *N*-terminus in CEM1 and at the *C*-terminus in CEM2. Closer examination of the sequence shows that while the glycine in CEM2 is positioned at the end of a densely positive charged region, in CEM1 the glycine is at the end of a markedly hydrophobic region. Additionally, glycine is known to have a good helix stabilizing effect at the *N*-terminal of helices [34].

3.5. Hydrodynamic diameters and ζ-potential of LUV

The hydrodynamic diameters and ζ-potential of the LUV in the absence and in the presence of increasing concentrations of CEM1 and CEM2 were evaluated (Fig. 3). Regarding their preparation, the size of DMPC and DMPG LUV was approximately 100 nm. In the presence of both peptides, DMPC LUV (Fig. 3A) exhibited a narrow size distribution with a mean diameter of approximately 80–110 nm, with a polidispersity below 0.1, suggesting that the peptides do not influence the mammalian cell membrane model even at high peptide concentration. However, the interaction of both peptides with DMPG LUV (Fig. 3B) induced pronounced changes on hydrodynamic mean diameters, especially at higher peptide concentrations. In fact, the hydrodynamic mean diameters of DMPG LUV in the presence of both peptides showed a heterogeneous size distribution with a hydrodynamic mean diameter varying between approximately 120 nm for 5 μM and 600 nm for 40 μM. The higher polydispersity values (>0.15) obtained in association with the higher mean diameter sizes for higher peptide concentrations point to the presence of a heterogeneous population, and the presence of aggregates. In fact, evaluation of the size distribution shows a small population of ~1.4 μm (Supplement 1D), which reflects the presence of aggregates in the sample. This observation could be due to the aggregation of membrane-bound peptide monomers, which has been reported to be associated to the formation of a pore complex involved in the disruption of bilayers [35]. The effect of the peptides on the membrane models was also evaluated by studying the changes in the particles charge (Fig. 4). The zeta potential of DMPC LUV was -6 ± 4 mV (Fig. 4A). When the peptides were present, the charge did not suffer significant modification (Fig. 4A). On the other hand, the results obtained demonstrate a higher charge variation for DMPG membrane model to more positive values (Fig. 4B). In fact, the zeta potential of DMPG LUV was -35 ± 3 mV, varying for more positive zeta potential values, reaching values of -18 ± 1 and -12 ± 2 mV for 40 μM of CEM1 and CEM2, respectively. These results support the establishment of electrostatic interactions between the positively charged amino acids, namely lysine, and the polar head groups of the phospholipids. In addition, it is well-known that zeta potential is a powerful technique to quantify peptide:lipid interactions, being the binding of the AMP to the membrane mainly attributed to electrostatic interactions between the peptide and the lipid head groups [36]. Regarding the similar variation of charge in the presence of DMPG LUV for both peptides CEM1 and CEM2, substantial differences between the peptides binding to the bacterial membrane are not expected.

3.6. LUV biophysical parameters

DLS using the count rate is a simple and reproducible technique to determine the biophysical parameters of the membrane, including T_m and cooperativity [28].

The biophysical parameters *Tm* and cooperativity of DMPC and DMPG LUV were studied in the absence and in the presence of CEM1 and CEM2 at two distinct concentrations: a high peptide concentration, 40 μM, far above the MIC for CEM1 against *P. aeruginosa* ((4–8 μg/mL)/(2.9–5.7 μM)) but still below the MIC for CEM2 ((128–265 μg/mL)/(94–194 μM)) and a low peptide concentration, 7.3 μM, just above the MIC for CEM1.

The analysis of Table 3, reveals that for high peptide concentrations the T_m obtained is consistent with previous reported studies [20]. Results show that both peptides have a negligible influence on the DMPC LUV main phase transition temperature. On the other hand, both peptides have a wide effect on DMPG LUV biophysical properties, which is

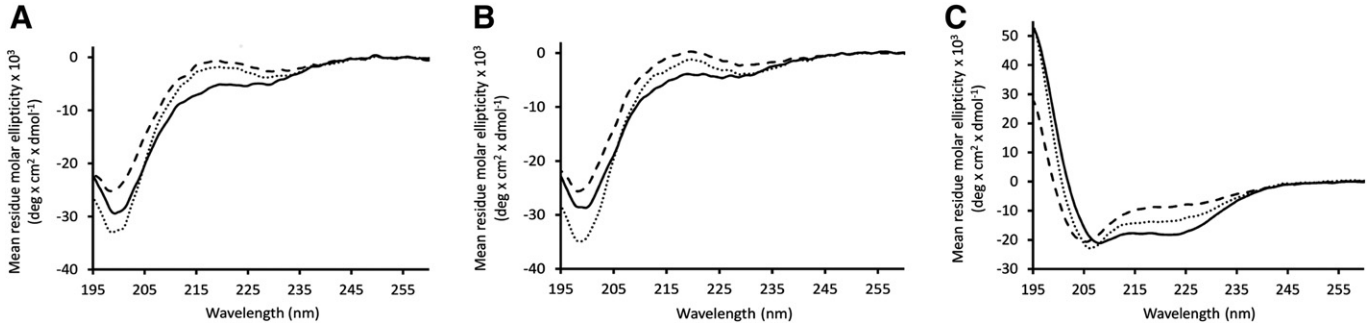

Fig. 2. CD spectra of peptides CEM1 (dotted line), CEM2 (dashed line) and MSI-78 (solid line) (40 μM) were acquired in aqueous buffer (A) and in the presence of DMPC (B) and DMPG (C) 5 mM LUV, corresponding to a peptide:lipid molar ratio of 1:125.

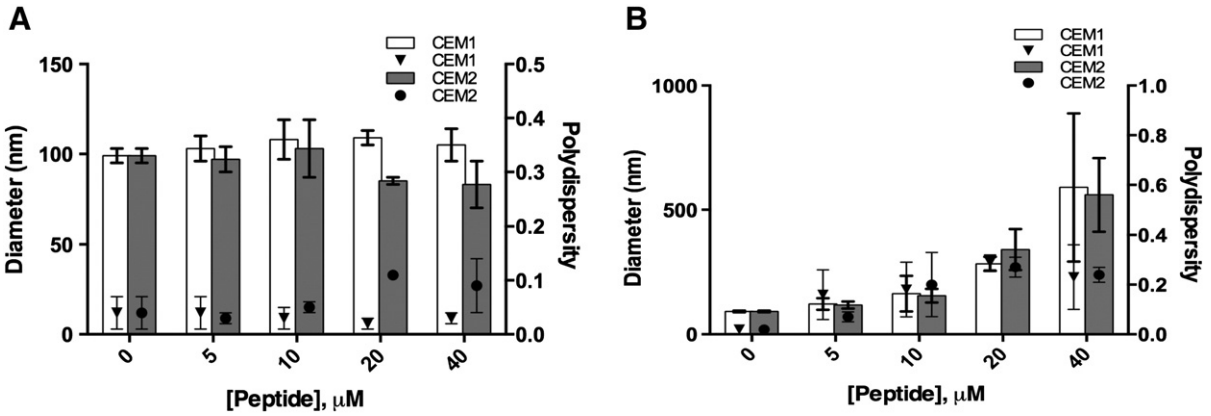

Fig. 3. Size and polydispersity index of DMPC (A) and DMPG (B) in the absence and in the presence of AMPs (5, 10, 20 and 40 μM).

especially pronounced in the case of CEM2. In fact, CEM1 lowered the T_m of DMPG LUV by roughly 3.0 °C. In the presence of CEM2, the effect on membrane fluidization is even more pronounced since the T_m remarkably drops approximately 7.0 °C. Furthermore, this result is followed by a substantial decrease in the cooperativity of the lipid, indicating that the peptide may form lipid patches due to the establishment of electrostatic interactions with the negatively charged phospholipids of the bacterial membrane model or it may be located buried in the lipid bilayer (Table 3). These results, point to a more pronounced effect of the less effective peptide (CEM2) on the biophysical properties of the bacterial cell membrane model when high concentrations of peptide are used. However, according to the *in vitro* biological assays conditions, *i.e.*, using a concentration of peptide slightly above the MIC of CEM1 for *P. aeruginosa*, which is markedly lower than the experimental MIC obtained for CEM2, provides evidence that CEM1 is the only peptide that produces changes on the biophysical properties of the membrane model (Table 4). In fact, CEM1 induces a lowering of the T_m corresponding to a fluidization of the membrane. Moreover, CEM1 at low concentration decreases the cooperativity of the DMPG LUV main phase transition, which may be related with the formation of lipid patches and/or strong internalization of the peptide in the lipid bilayer. On the other hand, in the presence of CEM2 the biophysical properties of the bacterial membrane model only suffer a slight change in terms of cooperativity of the main phase transition, with preservation of membrane fluidity.

4. Discussion

This study aimed at developing new short 12-mer AMP (CEM) derived from the well-studied MSI-78 by following a strategy of reducing the size by truncating the *C* and/or *N*-termini spanning the entire peptide by 1-aa shift. It has been previously shown that reasonable potency and spectrum of activity could be attained by short AMPs in comparison to longer ones [17,37–39]. According to the predictive algorithms, all CEM peptides were classified as AMPs. This is correct for most peptides, as they are active against *P. aeruginosa* with exception for CEM3 and CEM7 for the tested concentrations. However for these peptides, predictive tools do not seem to be suitable to foresee efficient antimicrobial activity for gram-positive bacteria.

Comparing the results obtained for the CEM dodecapeptides, it can also be concluded that the *C*-terminal part of the peptide MSI-78 has an important role in the antimicrobial activity as peptides covering this region consistently displayed some antimicrobial activity. This might be related to the high aliphatic index of these peptides.

Our studies show that shortening MSI-78 to a 12-mer peptide leads in general to loss of antimicrobial activity, which is more pronounced for gram-positive bacteria *S. aureus*, this effect is probably due to the positive charge reduction, while MSI-78 has a net charge of +9, CEM peptides have charges comprised between +4 and +6.

Nevertheless, CEM1, covering the first 12 amino acids of the MSI-78 peptide, stood out as a good candidate to fight *P. aeruginosa* infection and potentially *S. epidermidis* infection. CEM1 was selective towards bacteria as evaluated by hemolysis assays in agreement with an observed preferential interaction towards negatively charged bacterial membrane models, in contrast to the mammalian membrane models. Interestingly, the shift of only one glycine from the first position (*N*-terminus) in CEM1 to the last position (*C*-terminus) in peptide CEM2 diminished antimicrobial activity significantly. This was not expected, as glycine is the smallest amino acid and not charged, being usually used as spacer due to its neutrality. In addition, CEM1 and CEM2 do not

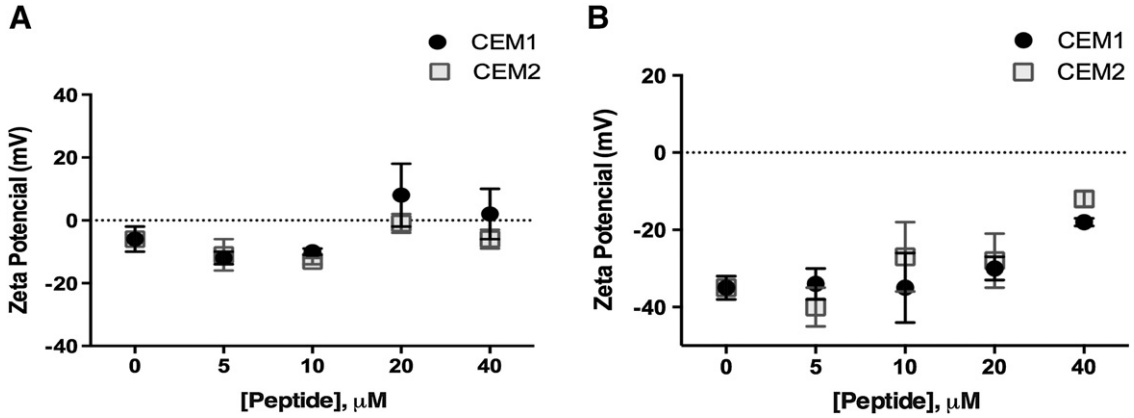

Fig. 4. Zeta potential of DMPC (A) and DMPG LUV (B) in the absence and in the presence of CEM1 and CEM2 (5, 10, 20 and 40 μM).

Table 3
Values of main phase transition temperature (T_m) and cooperativity (B) determined by DLS and obtained for DMPC and DMPG LUV (500 μM, pH 7.4) in the absence and in the presence of AMPs (40 μM).

	T_m	Cooperativity (B)
DMPC	24.4 ± 0.2	347 ± 34
DMPC + CEM1	23.5 ± 0.6	254 ± 54
DMPC + CEM2	23.9 ± 1.2	217 ± 61
DMPG	24.1 ± 0.5	233 ± 5
DMPG + CEM1	20.8 ± 0.1	438 ± 54
DMPG + CEM2	16.7 ± 1.8	102 ± 11

show differences in the most common features related to antimicrobial activity (Table 1). In order to understand their mechanism of action CEM1 and CEM2 were studied regarding their interactions with mammalian and bacterial cell membrane models. Our studies show that both peptides interact preferentially with the bacterial cell membrane models (negatively charged LUV-DMPG), which is consistent with the cytotoxicity studies. Concerning their distinct interaction with DMPG LUV, differences between CEM1 and CEM2 were only detected at low peptide concentrations. In opposition to CEM2, CEM1 induced pronounced changes on the biophysical parameters of DMPG LUV in a concentration that is slightly above the MIC for *P. aeruginosa*. These results show that interactions of CEM1 and CEM2 with membrane models are highly dependent on peptide concentrations. This dependence on AMP concentration related to the interaction with bacterial membranes strongly suggests that bacterial membrane binding facilitates nucleation-dependent AMP aggregation. This aggregation explains the larger mean hydrodynamic diameter obtained in the case of DMPG LUV for higher AMP concentrations. Nevertheless, as the molar ratios peptide:lipid are not comparable between antimicrobial activity tests and biophysical studies with LUV, a cautious analysis of the results has to be done.

A proposed mechanism for the interaction of CEM1 with bacterial membranes initiates with peptide binding to the membrane surface through electrostatic interactions, followed by the insertion of the positively charged residues into the interfacial region. Interaction of the peptides with the bacterial membranes results in changes of the peptides conformation from random coils to α-helices, causing local perturbations in the phospholipid headgroup region of the membrane and consequently bacterial cell death as previously described [40]. According to this, for peptides with the same size, the disturbance in membrane for the same AMP concentration will be higher with an increment of the helix dynamics [40,41]. Therefore, the higher percentage of α-helical conformation exhibited by CEM1 in contrast to CEM2 will be responsible for a more pronounced protein-phospholipid bacterial membrane interaction mediated by dynamic processes, for example, the rotational motion, wobbling, tilting, or bending of the helix [40]. The preferential interaction with anionic *vs* zwitterionic lipids has been also demonstrated for the template peptide MSI-78 [42], which due to the electrostatic interactions between the positively charged amino acids and the anionic lipid headgroups may lead to peptide conformational changes, creating hydrophobic patches in its structure, which favor the AMP insertion within the lipid bilayers. This insertion and consequently bacterial membrane model disruption was proven to be concentration-dependent as well, as described in the case of MSI-78 [42].

Table 4
Values of main phase transition temperature (T_m) and cooperativity (B) determined by DLS and obtained for DMPC and DMPG LUV (500 μM, pH 7.4) in the absence and in the presence of AMPs (7.3 μM).

	T_m	Cooperativity (B)
DMPG	24.1 ± 0.5	233 ± 5
DMPG + CEM1	21.4 ± 1.2	185 ± 10
DMPG + CEM2	23.1 ± 0.5	292 ± 62

This study is also an attempt to understand structure–antimicrobial activity relationship of designed AMPs. Other studies have addressed the possible effects of shortening AMPs, Deslouches and co-workers have reported that in peptides solely made from Arg and Val residues, improved antimicrobial activity is dependent on peptide length and conclude that a minimum length of 15 residues is required for significant antimicrobial activity [43]. These authors argue that hydrophilic and hydrophobic regions with increased length could explain the better performance of longer peptides, which could be an explanation for the loss of activity for the 12-mer MSI-78 derivatives. Zelezetsky and colleagues have shown that peptides as short as 14 residues lose their antimicrobial activity despite their adequate structure and sufficient charge [29]. In addition, shorter peptides could negatively influence the formation of an α-helix, the conformation that MSI-78 acquires when interacting with bacterial membranes. In fact, loss of propensity to form helices has been associated to a reduction of peptides spectrum of activity [43]. Overall, this study provides indications on possible strategies and consequences on the rational design of short, truncated peptides. Specifically the importance of preserving secondary conformation and exposition of positively charged residues.

As future perspective we could envisage the use of CEM1 in the treatment of *P. aeruginosa* related infections such as cystic fibrosis and other infections caused by gram-negative bacteria.

Acknowledgements

This work was financed by FCT (Fundação para a Ciência e Tecnologia) through Portuguese funds and funds provided by FEDER through the Programa Operacional Factores de Competitividade (COMPETE) in the framework of the projects FCOMP-01-0124-FEDER-009400 (PTDC/CTM/101484/2008), PEst-C/SAU/LA0002/2013, PEst-C/QUI/UI0081/2013 and the grants: SFRH/BPD/79439/2011 (Claudia Monteiro), SFRH/BPD/99124/2013 (Marina Pinheiro), SFRH/BD/72471/2010 (Fabíola Costa) and SFRH/BD/89001/2012 (Catarina Seabra).

The authors would like to thank to Centro Hospitalar de São João, EPE, Porto, for the human buffy coats.

References

[1] A.J. Alanis, Resistance to antibiotics: are we in the post-antibiotic era? Arch. Med. Res. 36 (2005) 697–705.
[2] E. Andres, J.L. Dimarcq, Cationic antimicrobial peptides: update of clinical development, J. Intern. Med. 255 (2004) 519–520.
[3] J. Cruz, C. Ortiz, F. Guzman, R. Fernandez-Lafuente, R. Torres, Antimicrobial peptides: promising compounds against pathogenic microorganisms, Curr. Med. Chem. 21 (20) (2014) 2299–2321.
[4] D. Fitzgerald-Hughes, M. Devocelle, H. Humphreys, Beyond conventional antibiotics for the future treatment of methicillin-resistant *Staphylococcus aureus* infections: two novel alternatives, FEMS Immunol. Med. Microbiol. 65 (2012) 399–412.
[5] F. Costa, I.F. Carvalho, R.C. Montelaro, P. Gomes, M.C. Martins, Covalent immobilization of antimicrobial peptides (AMPs) onto biomaterial surfaces, Acta Biomater. 7 (2011) 1431–1440.
[6] J.P. Powers, R.E. Hancock, The relationship between peptide structure and antibacterial activity, Peptides 24 (2003) 1681–1691.
[7] R.M. Epand, H.J. Vogel, Diversity of antimicrobial peptides and their mechanisms of action, Biochim. Biophys. Acta 1462 (1999) 11–28.
[8] M.R. Yeaman, N.Y. Yount, Mechanisms of antimicrobial peptide action and resistance, Pharmacol. Rev. 55 (2003) 27–55.
[9] Y. Ge, D.L. MacDonald, K.J. Holroyd, C. Thornsberry, H. Wexler, M. Zasloff, In vitro antibacterial properties of pexiganan, an analog of magainin, Antimicrob. Agents Chemother. 43 (1999) 782–788.
[10] B.A. Lipsky, K.J. Holroyd, M. Zasloff, Topical versus systemic antimicrobial therapy for treating mildly infected diabetic foot ulcers: a randomized, controlled, double-blinded, multicenter trial of pexiganan cream, Clin. Infect. Dis. 47 (2008) 1537–1545.
[11] L.M. Gottler, A. Ramamoorthy, Structure, membrane orientation, mechanism, and function of pexiganan—a highly potent antimicrobial peptide designed from magainin, Biochim. Biophys. Acta 1788 (2009) 1680–1686.
[12] M.G. Habets, M.A. Brockhurst, Therapeutic antimicrobial peptides may compromise natural immunity, Biol. Lett. 8 (2012) 416–418.
[13] A. Tossi, L. Sandri, A. Giangaspero, Amphipathic, alpha-helical antimicrobial peptides, Biopolymers 55 (2000) 4–30.
[14] R.E. Hancock, H.G. Sahl, Antimicrobial and host-defense peptides as new anti-infective therapeutic strategies, Nat. Biotechnol. 24 (2006) 1551–1557.

[15] M. Pasupuleti, A. Schmidtchen, A. Chalupka, L. Ringstad, M. Malmsten, End-tagging of ultra-short antimicrobial peptides by W/F stretches to facilitate bacterial killing, PLoS ONE 4 (2009) e5285.
[16] M. Bastos, G. Bai, P. Gomes, D. Andreu, E. Goormaghtigh, M. Prieto, Energetics and partition of two cecropin-melittin hybrid peptides to model membranes of different composition, Biophys. J. 94 (2008) 2128–2141.
[17] D. Andreu, J. Ubach, A. Boman, B. Wahlin, D. Wade, R.B. Merrifield, H.G. Boman, Shortened cecropin A-melittin hybrids. Significant size reduction retains potent antibiotic activity, FEBS Lett. 296 (1992) 190–194.
[18] O.G. Mouritsen, Model answers to lipid membrane questions, Cold Spring Harbor Perspect. Biol. 3 (2011) a004622.
[19] R.M. Hatfield, L.W. Fung, Molecular properties of a stratum corneum model lipid system: large unilamellar vesicles, Biophys. J. 68 (1995) 196–207.
[20] M. Pinheiro, M. Arede, C. Nunes, J.M. Caio, C. Moiteiro, M. Lucio, S. Reis, Differential interactions of rifabutin with human and bacterial membranes: implication for its therapeutic and toxic effects, J. Med. Chem. 56 (2013) 417–426.
[21] N. Ilic, M. Novkovic, F. Guida, D. Xhindoli, M. Benincasa, A. Tossi, D. Juretic, Selective antimicrobial activity and mode of action of adepantins, glycine-rich peptide antibiotics based on anuran antimicrobial peptide sequences, Biochim. Biophys. Acta 1828 (2013) 1004–1012.
[22] S.C. Lopes, C. Ribeiro, P. Gameiro, A new approach to counteract bacteria resistance: a comparative study between moxifloxacin and a new moxifloxacin derivative in different model systems of bacterial membrane, Chem. Biol. Drug Des. 81 (2013) 265–274.
[23] R.M. Epand, R.F. Epand, Domains in bacterial membranes and the action of antimicrobial agents, Mol. BioSyst. 5 (2009) 580–587.
[24] M. Brandt, S. Gammeltoft, K. Jensen, Microwave heating for solid-phase peptide synthesis: general evaluation and application to 15-mer phosphopeptides, Int. J. Pept. Res. Ther. 12 (2006) 349–357.
[25] I. Wiegand, K. Hilpert, R.E. Hancock, Agar and broth dilution methods to determine the minimal inhibitory concentration (MIC) of antimicrobial substances, Nat. Protoc. 3 (2008) 163–175.
[26] P. Luo, R.L. Baldwin, Mechanism of helix induction by trifluoroethanol: a framework for extrapolating the helix-forming properties of peptides from trifluoroethanol/water mixtures back to water, Biochemistry 36 (1997) 8413–8421.
[27] F. Barbato, G. di Martino, L. Grumetto, M.I. La Rotonda, Prediction of drug–membrane interactions by IAM-HPLC: effects of different phospholipid stationary phases on the partition of bases, Eur. J. Pharm. Sci. 22 (2004) 261–269.
[28] N. Michel, A.S. Fabiano, A. Polidori, R. Jack, B. Pucci, Determination of phase transition temperatures of lipids by light scattering, Chem. Phys. Lipids 139 (2006) 11–19.
[29] I. Zelezetsky, A. Tossi, Alpha-helical antimicrobial peptides—using a sequence template to guide structure–activity relationship studies, Biochim. Biophys. Acta 1758 (2006) 1436–1449.
[30] N.P. Chongsiriwatana, T.M. Miller, M. Wetzler, S. Vakulenko, A.J. Karlsson, S.P. Palecek, S. Mobashery, A.E. Barron, Short alkylated peptoid mimics of antimicrobial lipopeptides, Antimicrob. Agents Chemother. 55 (2011) 417–420.
[31] Y. Zhang, H. Zhao, G.Y. Yu, X.D. Liu, J.H. Shen, W.H. Lee, Structure–function relationship of king cobra cathelicidin, Peptides 31 (2010) 1488–1493.
[32] A. Mecke, D.K. Lee, A. Ramamoorthy, B.G. Orr, M.M. Banaszak Holl, Membrane thinning due to antimicrobial peptide binding: an atomic force microscopy study of MSI-78 in lipid bilayers, Biophys. J. 89 (2005) 4043–4050.
[33] A. Ramamoorthy, S. Thennarasu, D.K. Lee, A. Tan, L. Maloy, Solid-state NMR investigation of the membrane-disrupting mechanism of antimicrobial peptides MSI-78 and MSI-594 derived from magainin 2 and melittin, Biophys. J. 91 (2006) 206–216.
[34] J.S. Richardson, D.C. Richardson, Amino acid preferences for specific locations at the ends of alpha helices, Science 240 (1988) 1648–1652.
[35] S. Thennarasu, D.K. Lee, A. Tan, U. Prasad Kari, A. Ramamoorthy, Antimicrobial activity and membrane selective interactions of a synthetic lipopeptide MSI-843, Biochim. Biophys. Acta 1711 (2005) 49–58.
[36] J.M. Freire, M.M. Domingues, J. Matos, M.N. Melo, A.S. Veiga, N.C. Santos, M.A. Castanho, Using zeta-potential measurements to quantify peptide partition to lipid membranes, Eur. Biophys. J. 40 (2011) 481–487.
[37] H. Ulvatne, S. Karoliussen, T. Stiberg, O. Rekdal, J.S. Svendsen, Short antibacterial peptides and erythromycin act synergically against Escherichia coli, J. Antimicrob. Chemother. 48 (2001) 203–208.
[38] S.Y. Shin, K.S. Hahm, A short alpha-helical antimicrobial peptide with antibacterial selectivity, Biotechnol. Lett. 26 (2004) 735–739.
[39] W.L. Zhu, K.S. Hahm, S.Y. Shin, Cell selectivity and mechanism of action of short antimicrobial peptides designed from the cell-penetrating peptide Pep-1, J. Pept. Sci. 15 (2009) 569–575.
[40] M.A. Kol, A.I. de Kroon, J.A. Killian, B. de Kruijff, Transbilayer movement of phospholipids in biogenic membranes, Biochemistry 43 (2004) 2673–2681.
[41] C.C. Forbes, K.M. DiVittorio, B.D. Smith, Bolaamphiphiles promote phospholipid translocation across vesicle membranes, J. Am. Chem. Soc. 128 (2006) 9211–9218.
[42] P. Yang, A. Ramamoorthy, Z. Chen, Membrane orientation of MSI-78 measured by sum frequency generation vibrational spectroscopy, Langmuir 27 (2011) 7760–7767.
[43] B. Deslouches, S.M. Phadke, V. Lazarevic, M. Cascio, K. Islam, R.C. Montelaro, T.A. Mietzner, De novo generation of cationic antimicrobial peptides: influence of length and tryptophan substitution on antimicrobial activity, Antimicrob. Agents Chemother. 49 (2005) 316–322.